Unmanned Systems, Vol. 5, No. 4 (2017) 209–221
© World Scientific Publishing Company
DOI: 10.1142/S2301385017400052

Unmanned Systems
http://www.worldscientific.com/worldscinet/us

Adaptive Sliding Mode Fault-Tolerant Control for an Unmanned Aerial Vehicle

Ban Wang*, Youmin Zhang†

Department of Mechanical, Industrial and Aerospace Engineering, Concordia University, 1455 de Maisonneuve Blvd. W., Montreal, Quebec H3G 1M8, Canada

Sliding mode control (SMC) is known as a robust control method to maintain system performance and keep it insensitive to system uncertainties. To achieve this objective, the knowledge of the uncertainty bound is usually needed, but sometimes it could be a hard task. Hence, the adaptive technology is introduced to be synthesized with SMC. In this paper, a novel adaptive SMC (ASMC) scheme is proposed to accommodate system uncertainties caused by actuator faults. An integral sliding mode controller is used as the baseline controller. When actuator faults occur, there is no need to know the exact bound of the uncertainties in control effectiveness matrix. The post-fault control effectiveness matrix can be estimated by the proposed adaptive control scheme, and the control inputs will be changed accordingly. In such a way, the robustness of the controller to actuator faults is improved. With the help of adaptive change of both continuous and discontinuous control parts, a minimum value of the discontinuous control gain can be guaranteed. In this case, the resulting control effort is reduced accordingly to avoid control chattering effect. Owing to the minimized control effort to accommodate uncertainties compared to the conventional SMC, the proposed ASMC can still maintain the system performance when severer faults occur. The effectiveness of the developed algorithm is demonstrated by the simulation results based on an unmanned quadrotor helicopter under various faulty conditions.

Keywords: Actuator fault; adaptive sliding mode control; fault-tolerant control; quadrotor helicopter; unmanned aerial vehicle.

1. Introduction

Unmanned aerial vehicles (UAVs) are increasingly becoming a topic of interest, not only in military applications but also extended into civilian applications [1–6]. In order to make wider use of UAVs and make them more intelligent for practical applications such as fire detecting and fighting, power-line inspection, and surveillance, safety is a big issue to be considered [7, 8]. More recently, the fault-tolerant capability of unmanned systems has begun to draw more and more attention in both industrial and academic communities, due to the increased demands for safety and reliability [9–11]. As argued in [12, 13], the increasing demands for safety, reliability, and high system performance have stimulated research in the area of fault-tolerant control (FTC) beneficial from the new developments in control theory, computer technology, actuator, and sensor techniques. Fault-tolerant capability is an important feature for safety-critical systems such as UAVs, chemical processing plants, nuclear power plants, etc. The main objective is to maintain the overall system stability and acceptable degree of performance in the presence of faults in the system [12]. From the point of fault occurrence location, faults can be classified into actuator faults, sensor faults, and other system component faults [12, 14]. Partial loss of control effectiveness of actuator is a common fault occurring in aircraft systems. Since the actuator plays an important role of connecting control signals to physical movements of the system to accomplish specific objectives, actuator fault is considered in this paper. One way to accommodate this kind of fault is to use the robustness of the control system which

Received 1 September 2016; Revised 24 June 2017; Accepted 24 June 2017; Published 1 November 2017. This paper was recommended for publication in its revised form by editor-in-chief Ben M. Chen.
Email Addresses: *npuwangban@gmail.com, †ymzhang@encs.concordia.ca,
†Corresponding author.

does not require on-line detection of fault as opposed to active FTC system [12, 15, 16]. This so-called robust controller treats faults as uncertainties in the system, which can be incorporated in controller design [17]. Therefore, a trade-off between system performance and robustness is unavoidable. Moreover, if a large fault is considered during the design stage, it will lead to an unacceptable performance in normal (fault-free) conditions, due to the big trade-off for taking such a large uncertainty into consideration. Since real systems mostly work under normal conditions and fault does not occur all the time, the consideration of fault during design stage will sacrifice certain degree of performance.

Sliding mode control (SMC) is an approach to design robust control systems dealing with large uncertainties with discontinuous control strategy which can demonstrate invariance to so-called matched uncertainties while on a reduced order sliding surface [18, 19]. More precisely, SMC synthesizes one design parameter in the discontinuous control part to deal with uncertainties which leads to significant control performance in both fault-free and faulty conditions. Studies by Wang *et al.* [20], Li *et al.* [21], Alwi *et al.* [22], and Hamayun *et al.* [23] show some of the most recent researches on reconfigurable flight control using SMC techniques. The property of insensitivity to parametric uncertainties makes SMC as one of the most promising approaches [24]. However, for using this traditional SMC, the bound of uncertainty is always needed at the design stage. For some applications, fault could occur at any time with unknown magnitude, and it is hard to obtain the exact uncertainty bound in advance. This stimulates a new control strategy, which incorporates adaptive schemes into SMC to accommodate faults without knowing the exact uncertainty bound [25–27]. In [27], with the proposed adaptive SMC (ASMC), it shows a good tracking performance when an actuator fault occurs in the system. However, as the fault becomes larger, a bigger tracking error occurs, and the system performance cannot be maintained anymore. This is because, the considered actuator fault is related to the uncertainty in control effectiveness matrix, and after a fault occurs, the control effectiveness matrix should be changed correspondingly. The existing ASMC for accommodating actuator fault only incorporates the adaptation parameter into the discontinuous control part. However, when a fault occurs, the continuous control part, i.e. the equivalent control part, should also be changed. To solve this problem, the estimation of the post-fault control effectiveness matrix needs to be obtained properly.

In this paper, a novel ASMC with integral type sliding surface is introduced. An adaptive scheme is synthesized to estimate the post-fault control effectiveness matrix, which has an effect on both continuous and discontinuous control parts. Like other ASMC algorithms, the exact value of the uncertainty bound is not required to deal with the uncertainty caused by an actuator fault. Compared to the existing ASMC schemes in the literature, the main contributions of the proposed control scheme are listed below. Firstly, the proposed control scheme can adaptively generate appropriate control inputs without merely relying on the robustness generated from the discontinuous control strategy, i.e. the equivalent control part will also be changed adaptively to achieve a better tracking performance. Secondly, due to the lesser use of the discontinuous control strategy, the control effort is significantly reduced which means larger faults can be tolerated, and control chattering effect is also pacified.

The rest of this paper is organized as follows. In Sec. 2, an ASMC is proposed, and for comparison, a traditional SMC with bounded uncertainty in control effectiveness matrix is introduced as well. The modeling of an unmanned quadrotor helicopter is presented in Sec. 3. In Sec. 4, simulation results are presented to verify the effectiveness of the proposed algorithm. Finally, general conclusions of this paper are summarized in Sec. 5.

2. Adaptive Sliding Mode Controller Design

2.1. *Problem formulation*

Consider a general uncertain linear system subject to actuator faults of the form:

$$\dot{x}(t) = x_1(t), \tag{1}$$

$$\dot{x}_1(t) = Ax(t) + B_0(I - H(t))u(t), \tag{2}$$

where $A \in \mathbb{R}^{n\times n}$ is the state matrix, $B_0 \in \mathbb{R}^{n\times m}$ with $1 \leq m \leq n$ is the control effectiveness matrix, and both of them are known. $u(t) \in \mathbb{R}^m$ is the control input vector and the diagonal matrix $H(t) = \mathrm{diag}([h_1(t), \ldots, h_m(t)])$ represents the loss of control effectiveness in the actuators, where $h_j(t)$ is scalar satisfying $0 \leq h_j(t) < 1$. Thus, if $h_j(t) = 0$, the jth actuator works perfectly, whereas if $h_j(t) > 0$, the jth actuator suffers some level of fault. Note that the state $x(t)$ is assumed measurable.

In order to make the fault clear and easy to present, one can define $\Delta B = -H(t)B_0$, then Eq. (2) can be rewritten as

$$\dot{x}_1(t) = Ax(t) + (B_0 + \Delta B)u(t), \tag{3}$$

$$B = B_0 + \Delta B, \tag{4}$$

where B_0 is the control effectiveness matrix before the faults occur.

Assumption 2.1. rank $B_0 = m$.

Assumption 2.2. The pair (A, B_0) is controllable.

Remark 2.1. The actuator fault ΔB can be treated as a matched uncertainty and it satisfies the so-called matching condition:

$$\Delta B \in \mathrm{Im}\, B_0,$$

i.e. there exists a matrix $\gamma(t) \in \mathbb{R}^{m\times m}$, such that $\Delta B = B_0\gamma(t)$.

2.2. *Integral-type sliding surface design*

Typically, the design of a sliding mode controller is composed of two steps. The first step involves the design of a sliding surface, on which the system performance is maintained as expected. The second one is concerned with the selection of a control law that will make the sliding surface attractive to the system states. Once the sliding surface is reached, the states are kept in the close neighborhood of the sliding surface.

The integral sliding surface for the system is defined by the following set:

$$S = \{x(t) \in \mathbb{R}^n : \ \sigma(x(t), t) = 0\}. \tag{5}$$

The switching function $\sigma(x(t), t) \in \mathbb{R}^n$ is defined as

$$\sigma(x(t), t) = \sigma_0(x(t), t) + z, \tag{6}$$

$$\sigma_0(x(t), t) = C^T x(t), \tag{7}$$

where $C \in \mathbb{R}^n, \sigma_0(x(t), t)$ is the linear combination of the states, which is similar to the conventional sliding mode design. z includes the integral term and will be determined below.

First of all, assume that there is no fault, i.e. $\Delta B = 0$, then the ideal system can be given by the following equations:

$$\ddot{x}_0(t) = Ax_0(t) + B_0u_0(t), \tag{8}$$

$$x(t_0) = x_0(t_0), \tag{9}$$

where $x_0(t)$ denotes the state trajectory of the ideal system under control input $u_0(t)$.

The choice of z is determined by the following equations which guarantee that $\sigma(x_0(t), t_0) = 0$.

$$\dot{z} = -C^T(Ax(t) + B_0u_0(t)), \tag{10}$$

$$z(0) = -C^T x(t_0), \tag{11}$$

i.e.

$$z = -C^T\left[x(t_0) + \int_{t_0}^{t} (Ax(\tau) + B_0u_0(\tau))d\tau\right]. \tag{12}$$

Remark 2.2. The term $x(t_0) + \int_{t_0}^{t} (Ax(\tau) + B_0u_0(\tau))d\tau$ in Eq. (12) can be regarded as the trajectory of the ideal system under the nominal control input u_0. That is, the motion equation of the sliding mode coincides with that of the ideal system without perturbation.

Remark 2.3. With this definition of z, it is obtained that $\sigma(x(t_0), t_0) = \sigma_0(x(t_0), t_0) + z(0) = 0$. Thus, the system trajectory under integral SMC starts from the designed sliding surface and the reaching phase is eliminated accordingly in contrast with conventional SMC.

Now, the problem is to design a control law that, provided $x(t_0) = x_0(t_0)$, guarantees the identity $x(t) = x_0(t)$ for all the time $t \geq 0$. Then the control law can be formulated in the following form:

$$u(t) = u_0(t) + u_1(t), \tag{13}$$

where $u_0(t)$ is the continuous nominal control part to stabilize the ideal system, which is assumed to be fault-free and in absence of uncertainties as shown in Eq. (8), such that the ideal system follows a given trajectory with satisfactory accuracy. $u_1(t)$ is the discontinuous integral SMC part to compensate the perturbations that satisfy the matching condition in order to ensure the sliding motion.

Denoting $x_d(t)$ as the desired trajectory, another variable $\tilde{x}(t) = x(t) - x_d(t)$ can be defined. Then the sliding manifold is redefined as

$$\sigma(\tilde{x}(t), t) = \sigma_0 + z, \tag{14}$$

where

$$\sigma_0 = \tilde{x}(t) + \dot{\tilde{x}}(t), \tag{15}$$

$$\dot{z} = -\dot{\tilde{x}}(t) + K_1\dot{\tilde{x}}(t) + K_2\tilde{x}(t),$$

$$z(0) = -\tilde{x}(t_0) - \dot{\tilde{x}}(t_0), \tag{16}$$

with diagonal matrices K_1 and K_2 denoting design parameters.

2.3. *Fault-tolerant control with bounded uncertainty*

In this section, the traditional SMC is introduced to make a comparison with the proposed ASMC. Assume that the bound of the uncertainty is known during the design stage, and it is incorporated into the design of the discontinuous control gain. In this case, in order to compensate the presumed fault, the discontinuous control gain needs to be increased which will stimulate significant control effort.

Assumption 2.3. The uncertainty in control effectiveness matrix caused by an actuator fault is known within a certain margin and satisfies

$$\|\Delta B \cdot B_0^{+}\| < \beta < 1, \tag{17}$$

where B_0^+ is the pseudo inverse of B_0 defined by

$$B_0^+ = (B_0^T B_0)^{-1} B_0^T, \tag{18}$$

and β is a positive constant representing the upper bound of the uncertainty induced by an actuator fault.

In order to analyze the sliding motion associated with the switching surface in Eq. (14) in the presence of the actuator fault, the time derivative of the sliding manifold is computed as follows:

$$\dot{\sigma}(\tilde{x}(t), t) = \ddot{\tilde{x}}(t) + K_1\dot{\tilde{x}}(t) + K_2\tilde{x}(t). \tag{19}$$

Equalizing $\dot{\sigma}(\tilde{x}(t), t) = 0$ yields

$$u_0 = B_0^+(\ddot{x}_d(t) - K_1\dot{\tilde{x}}(t) - K_2\tilde{x}(t) - Ax(t)). \tag{20}$$

Then, substituting Eq. (20) into Eqs. (1) and (3) yields

$$\ddot{x}(t) = Ax(t) + BB_0^+(\ddot{x}_d(t) - K_1\dot{\tilde{x}}(t) - K_2\tilde{x}(t) - Ax(t)). \tag{21}$$

Remark 2.4. Note that in the case of no fault in the system ($\Delta B = 0$), there exists $(B_0 + \Delta B)B_0^+ = I$. Equation (21) becomes $\ddot{\tilde{x}}(t) + K_1\dot{\tilde{x}}(t) + K_2\tilde{x}(t) = 0$, so the sliding motion is achieved for the ideal system.

In the presence of fault, in order to maintain the sliding motion, the discontinuous part is added and designed as below:

$$u_1 = -B_0^+ K_c \mathrm{sign}(\sigma), \tag{22}$$

where K_c is a positive high gain matrix which makes the sliding surface attractive.

Theorem 1. *For the system described in Eqs.* (*1*) *and* (*2*), *assume that the uncertainty is bounded in Eq.* (*17*). *Then in a faulty condition for any* $h_j(t) > 0$, *by employing the following feedback control*:

$$\begin{aligned} u(t) = {} & B_0^+(\ddot{x}_d(t) - K_1\dot{\tilde{x}}(t) - K_2\tilde{x}(t) - Ax(t)) \\ & - B_0^+ K_c \mathrm{sign}(\sigma), \end{aligned} \tag{23}$$

the sliding motion will be achieved and maintained if

$$K_c \geq \frac{u^*\beta + \eta u^*/\|u^*\|}{1+\beta}, \tag{24}$$

where $u^* = \ddot{x}_d(t) - K_1\dot{\tilde{x}}(t) - K_2\tilde{x}(t) - Ax(t)$ *and* η *is a small positive constant.*

Proof. Substituting Eq. (23) into Eq. (19) gives

$$\begin{aligned} \dot{\sigma}(\tilde{x}(t), t) = {} & Ax(t) + BB_0^+(\ddot{x}_d(t) - K_1\dot{\tilde{x}}(t) - K_2\tilde{x}(t) \\ & - Ax(t)) - BB_0^+K_c\mathrm{sign}(\sigma) - \ddot{x}_d(t) \\ & + K_1\dot{\tilde{x}}(t) + K_2\tilde{x}(t). \end{aligned} \tag{25}$$

Consider the candidate Lyapunov function as

$$V(t) = \frac{1}{2}\sigma(\tilde{x}(t), t)^T\sigma(\tilde{x}(t), t). \tag{26}$$

The time derivative of the candidate Lyapunov function satisfies

$$\begin{aligned} \dot{V} = {} & \sigma Ax(t) + \sigma BB_0^+(\ddot{x}_d(t) - K_1\dot{\tilde{x}}(t) - K_2\tilde{x}(t) - Ax(t)) \\ & - \sigma BB_0^+K_c\mathrm{sign}(\sigma) - \sigma\ddot{x}_d(t) + \sigma K_1\dot{\tilde{x}}(t) + \sigma K_2\tilde{x}(t) \\ = {} & \sigma\Delta BB_0^+(\ddot{x}_d(t) - K_1\dot{\tilde{x}}(t) - K_2\tilde{x}(t) - Ax(t)) \\ & - \sigma K_c\mathrm{sign}(\sigma) - \sigma\Delta BB_0^+K_c\mathrm{sign}(\sigma). \end{aligned} \tag{27}$$

Since the loss of control effectiveness of actuator fault is considered here, the assumption $\|\Delta B \cdot B_0^+\| < \beta < 1$ holds. Therefore,

$$\begin{aligned} \dot{V} & \leq \|\sigma\|\beta(\ddot{x}_d(t) - K_1\dot{\tilde{x}}(t) - K_2\tilde{x}(t) - Ax(t)) \\ & \quad - \|\sigma\|K_c - \|\sigma\|\beta K_c \\ & = \|\sigma\|(u^*\beta - (1+\beta)K_c) \\ & \leq \frac{-\eta u^*\|\sigma\|}{\|u^*\|}. \end{aligned} \tag{28}$$

Thus, the system satisfies the standard η-reachability condition, which implies that the system can asymptotically track the desired trajectory and the sliding motion is maintained all the time. □

However, in order to account for the uncertainty, the control discontinuity is increased which may lead to control chattering. One can remove this condition by smoothing the control discontinuity in a thin boundary layer neighboring the switching surface:

$$\bar{B} = \{\tilde{x}, \|\sigma(\tilde{x}; t)\| \leq \Phi\}, \tag{29}$$

where Φ is the boundary layer thickness with positive value.

Accordingly, the feedback control law $u(t)$ becomes

$$\begin{aligned} u(t) = {} & B_0^+(\ddot{x}_d(t) - K_1\dot{\tilde{x}}(t) - K_2\tilde{x}(t) - Ax(t) \\ & - K_c\mathrm{sat}(\sigma/\Phi)), \end{aligned} \tag{30}$$

where the sat function is defined as follows:

$$\mathrm{sat}(\sigma/\Phi) = \begin{cases} \mathrm{sign}(\sigma), & \text{if } \|\sigma\| > \Phi \\ \sigma/\Phi, & \text{if } \|\sigma\| < \Phi \end{cases}. \tag{31}$$

2.4. *Adaptive fault-tolerant control*

As shown before, the integral SMC can achieve effective tracking performance in the presence of parametric uncertainties in control effectiveness matrix while avoiding exciting high-frequency dynamics. However, for some real applications, an actuator fault could occur in the system at any time, with unknown magnitude. It is hard to know the uncertainty bound in advance. This stimulates the authors to investigate the adaptive approach combined with SMC to accommodate the unknown uncertainty and fault. For large parametric uncertainties, which might cause significant control efforts, the adaptive sliding mode is also required to improve the control system performance.

Intuitively, the actuator fault is related to the control effectiveness matrix. When an actuator fault occurs, the corresponding control gain will change accordingly. Therefore, in order to be effective to accommodate the fault, merely increasing the discontinuous control gain is not enough. Because when the discontinuous control gain is increased, the related control effort will be increased, and the chattering phenomenon might be stimulated as well. Therefore, both the continuous and discontinuous control parts should be changed accordingly. In this section, instead of using the pre-fault control matrix B_0^+, the post-fault control effectiveness matrix $\hat{B}^+$ is used for deriving the control law. The adaptive scheme is then employed to estimate the post-fault control effectiveness matrix. In this case, when an actuator fault occurs, both the continuous and discontinuous control parts will be adaptively changed to compensate the fault more effectively (as shown in Fig. 1).

The sliding surface in Eq. (14) is employed, and the derivative of the sliding surface can be found in Eq. (19). Then the continuous control part is given by

$$u_0 = \hat{B}^+(\ddot{x}_d(t) - K_1\dot{\tilde{x}}(t) - K_2\tilde{x}(t) - Ax(t)), \qquad (32)$$

where $\hat{B}^+$ is the pseudo inverse of $\hat{B}$ given by

$$\hat{B}^+ = (\hat{B}^T\hat{B})^{-1}\hat{B}^T, \qquad (33)$$

and $\hat{B}$ is the available estimation of the post-fault control effectiveness matrix.

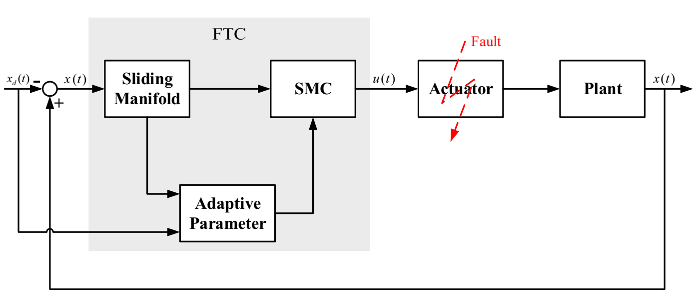

Fig. 1. Schematic of the proposed ASMC.

Theorem 2. *Define the adaptive law for estimating the uncertain control effectiveness matrix as*

$$\dot{\hat{B}}^{+} = [-\ddot{x}_d(t) + K_1\dot{\tilde{x}}(t) + K_2\tilde{x}(t) + Ax(t) + K_c\mathrm{sat}(\sigma/\Phi)]\sigma_\Delta, \qquad (34)$$

where $\sigma_\Delta = \sigma - \Phi\mathrm{sat}(\sigma/\Phi)$ *is the measurement of the algebraic distance between the current state and the boundary layer.*

Assume that after fault occurrence, the control effectiveness matrix B is unknown but constant

$$\Delta B = E, \qquad (35)$$

where E is a constant matrix.

Then, the system trajectory is guaranteed to remain on the sliding surface with the choice that,

$$K_c \geq \frac{\eta u^*}{\|u^*\|}. \qquad (36)$$

Remark 2.5. Compared to the discontinuous control gain K_c in the traditional SMC with bounded uncertainty, the one in the proposed ASMC is reduced due to the change of the continuous control part. In this case, the chattering effect is suppressed.

Proof. In order to ensure the sliding motion convergences to the boundary layer, a Lyapunov function is defined as follows:

$$V = \frac{1}{2}[\sigma_\Delta^T\sigma_\Delta + B(\hat{B}^+ - B^+)^T(\hat{B}^+ - B^+)]. \qquad (37)$$

When the sliding motion is inside the boundary layer, $\sigma_\Delta = 0$ holds, in this case the derivative of the Lyapunov function becomes

$$\dot{V} = 0. \qquad (38)$$

When it is outside the boundary layer, $\dot{\sigma}_\Delta = \dot{\sigma}$, and there exists

$$\dot{V} = \dot{\sigma}_\Delta\sigma_\Delta + B(\hat{B}^+ - B^+)\dot{\hat{B}}^{+}. \qquad (39)$$

Substituting Eqs. (25) and (34) into Eq. (39) gives

$$\begin{aligned}\dot{V} = {} & [Ax(t) + B\hat{B}^+(\ddot{x}_d(t) - K_1\dot{\tilde{x}}(t) - K_2\tilde{x}(t) - Ax(t)) \\ & - B\hat{B}^+K_c\mathrm{sat}(\sigma/\Phi) - \ddot{x}_d(t) + K_1\dot{\tilde{x}}(t) + K_2\tilde{x}(t)]\sigma_\Delta \\ & + B\hat{B}^+[-\ddot{x}_d(t) + K_1\dot{\tilde{x}}(t) + K_2\tilde{x}(t) + Ax(t)]\sigma_\Delta \\ & - BB^+[-\ddot{x}_d(t) + K_1\dot{\tilde{x}}(t) + K_2\tilde{x}(t) + Ax(t)]\sigma_\Delta \\ & + (B\hat{B}^+ - BB^+)K_c\mathrm{sat}(\sigma/\Phi)\sigma_\Delta. \end{aligned} \qquad (40)$$

Furthermore, it can be obtained that,

$$\begin{aligned}\dot{V} &= -K_c\mathrm{sat}(\sigma/\Phi)\sigma_\Delta \\ &\leq -K_c\|\sigma_\Delta\|. \end{aligned} \qquad (41)$$

Finally, with the physical control law obtained below

$$u(t) = -\hat{B}^{+}[\ddot{x}_d(t) + K_1\dot{\tilde{x}}(t) + K_2\tilde{x}(t) + Ax(t) + K_c\mathrm{sat}(\sigma/\Phi)], \tag{42}$$

the sliding motion is maintained all the time. □

Remark 2.6. Since the construction of the sliding surface is based on the tracking error of the concerned state and its derivative, and the desired sliding surface is defined as $\sigma = 0$, if the desired sliding surface can be achieved and maintained, it means that the tracking error and its derivative converge to zero. In this case, the stability and tracking performance of the original system can be maintained.

3. Modeling of an Unmanned Quadrotor Helicopter

The mathematical model of an unmanned quadrotor helicopter is described in this section, which will be used as a testbed for the demonstration of the developed algorithms. The quadrotor helicopter used in this paper is called Qball-X4, produced by Quanser. The quadrotor helicopter is very well modeled with four motors in a cross configuration. All the propellers' axes of rotation are fixed and parallel. Furthermore, they have fixed-pitch blades and their air flows point downwards. These considerations point out that the structure is quite rigid and the only thing that can vary is the speeds of the propellers. Each pair of opposite propellers turns the same way. The front and rear propellers rotate clockwise, and the left and right ones spin counter-clockwise (see Fig. 2) [28]. In this configuration, two opposite propellers contribute to the motion in x- and y-axes, respectively. Therefore, the rotations about these two axes can be decoupled.

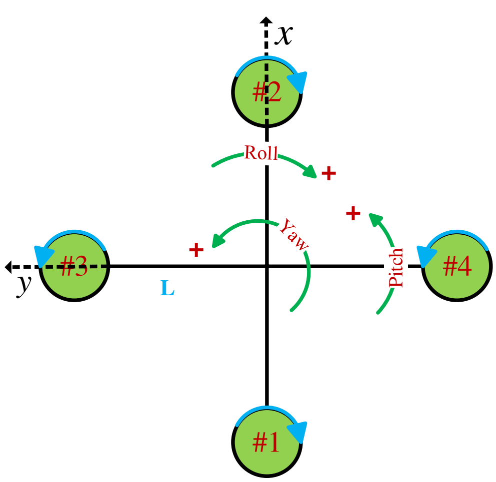

Fig. 2. Configuration of the unmanned quadrotor helicopter.

The relationship between the thrust T_i and the ith motor is given by [29]

$$T_i = K\frac{\omega}{s+\omega}u_i, \tag{43}$$

where K is a positive gain, ω is the actuator bandwidth, and u_i is the ith motor's PWM input.

In order to make it easier to model the actuator dynamics, a state variable ν is defined to represent the actuator dynamics

$$\nu_i = \frac{\omega}{s+\omega}u_i. \tag{44}$$

Thus, the thrust can be represented as:

$$T_i = K\nu_i. \tag{45}$$

The generated torque by each motor is defined as:

$$\tau_i = K_y\nu_i, \tag{46}$$

where K_y is a positive gain.

Therefore, the forces and moments along with each axis can be obtained as:

$$\begin{cases} u_z = K(\nu_1+\nu_2+\nu_3+\nu_4), \\ u_\phi = KL(\nu_3-\nu_4), \\ u_\theta = KL(\nu_1-\nu_2), \\ u_\psi = K_y(\nu_1+\nu_2-\nu_3-\nu_4), \end{cases} \tag{47}$$

where L is the distance between the propeller and the center of gravity of the quadrotor helicopter.

According to Newton's second law, the nonlinear dynamics of the quadrotor helicopter in hybrid-frame can be written as follows:

$$\begin{cases} \ddot{X} = (\cos\phi\sin\theta\cos\psi + \sin\phi\sin\psi)\dfrac{u_z}{m}, \\ \ddot{Y} = (\cos\phi\sin\theta\sin\psi - \sin\phi\cos\psi)\dfrac{u_z}{m}, \\ \ddot{Z} = (\cos\phi\cos\theta)\dfrac{u_z}{m} - g, \\ \dot{p} = \dfrac{I_{yy}-I_{zz}}{I_{xx}}qr + \dfrac{u_\phi}{I_{xx}}, \\ \dot{q} = \dfrac{I_{zz}-I_{xx}}{I_{yy}}pr + \dfrac{u_\theta}{I_{yy}}, \\ \dot{r} = \dfrac{I_{xx}-I_{yy}}{I_{zz}}pq + \dfrac{u_\psi}{I_{zz}}, \end{cases} \tag{48}$$

where I_{xx}, I_{yy} and I_{zz} is the inertial moment along with each axis, respectively, and m is the weight of the quadrotor. p is the roll angular rate, q is the pitch angular rate, and r is the yaw angular rate.

By now, the nonlinear model of the quadrotor helicopter has been obtained as shown in Eq. (48). However, in order to facilitate the controller design, the nonlinear dynamics should be simplified. Since the changes of roll and pitch angles can be assumed to be very small, the transfer matrix T_θ shown in Eqs. (49) and (50), which defines the relationship between the angular velocities in the body-fixed frame and those in the earth-fixed inertial frame, is very close to an identity matrix. Therefore, the angular velocities can be replaced directly by the Euler-angle rates as shown in Eq. (51). Associated parameters of the quadrotor helicopter used in the above equations are listed in Table 1.

$$\begin{bmatrix} p \\ q \\ r \end{bmatrix} = T_\Theta \begin{bmatrix} \dot{\phi} \\ \dot{\theta} \\ \dot{\psi} \end{bmatrix}. \tag{49}$$

$$T_\Theta = \begin{bmatrix} 1 & 0 & -\sin\theta \\ 0 & \cos\phi & \cos\theta\sin\phi \\ 0 & -\sin\phi & \cos\theta\cos\phi \end{bmatrix}. \tag{50}$$

$$\begin{cases} \ddot{X} = (\cos\phi\sin\theta\cos\psi + \sin\phi\sin\psi)\dfrac{u_z}{m}, \\ \ddot{Y} = (\cos\phi\sin\theta\sin\psi - \sin\phi\cos\psi)\dfrac{u_z}{m}, \\ \ddot{Z} = (\cos\phi\cos\theta)\dfrac{u_z}{m} - g, \\ \ddot{\phi} = \dfrac{I_{yy} - I_{zz}}{I_{xx}}\dot{\theta}\dot{\psi} + \dfrac{u_\phi}{I_{xx}}, \\ \ddot{\theta} = \dfrac{I_{zz} - I_{xx}}{I_{yy}}\dot{\phi}\dot{\psi} + \dfrac{u_\theta}{I_{yy}}, \\ \ddot{\psi} = \dfrac{I_{xx} - I_{yy}}{I_{zz}}\dot{\phi}\dot{\theta} + \dfrac{u_\psi}{I_{zz}}. \end{cases} \tag{51}$$

In order to linearize the mathematical model of the quadrotor for the controller design, the motion of the quadrotor is assumed to be close to the hover condition, yaw angle is fixed to zero ($\psi = 0$), and small angle changes occur for roll and pitch. Based on this trim condition, the linearized dynamic model of the quadrotor helicopter can be summarized as follows:

$$\begin{cases} \ddot{X} = g\theta, & \ddot{\phi} = \dfrac{u_\phi}{I_{xx}}, \\ \ddot{Y} = -g\phi, & \ddot{\theta} = \dfrac{u_\theta}{I_{yy}}, \\ \ddot{Z} = -g + \dfrac{u_z}{m}, & \ddot{\psi} = \dfrac{u_\psi}{I_{zz}}. \end{cases} \tag{52}$$

Thus, for the position and attitude control of the quadrotor helicopter, the state vector is defined as $x = [X\ Y\ Z\ \phi\ \theta\ \psi]^T$. In this case, the matrix A is a null matrix and matrix B_0 is calculated as follows:

$$B_0 = \begin{bmatrix} g & 0 & 0 & 0 & 0 & 0 \\ 0 & -g & 0 & 0 & 0 & 0 \\ 0 & 0 & K & K & K & K \\ 0 & 0 & 0 & 0 & \dfrac{KL}{I_{xx}} & -\dfrac{KL}{I_{xx}} \\ 0 & 0 & \dfrac{KL}{I_{yy}} & -\dfrac{KL}{I_{yy}} & 0 & 0 \\ 0 & 0 & \dfrac{K_y}{I_{zz}} & \dfrac{K_y}{I_{zz}} & -\dfrac{K_y}{I_{zz}} & \dfrac{K_y}{I_{zz}} \end{bmatrix}. \tag{53}$$

Table 1. System parameters.

Parameter	Description	Value
K	Thrust gain	120 N
ω	Motor bandwidth	15 rad/sec
M	Mass	1.4 kg
L	Distance	0.2 m
K_y	Torque gain	4 N·m
I_{xx}	Inertial moment along x axis	0.03 kg·m^2
I_{yy}	Inertial moment along y axis	0.03 kg·m^2
I_{zz}	Inertial moment along z axis	0.04 kg·m^2

4. Simulation Results

In this section, in order to demonstrate the performance of the proposed ASMC, simulations based on the unmanned Qball-X4 quadrotor helicopter under different faulty scenarios are carried out. Firstly, the longitudinal motion of the quadrotor helicopter is considered to track a pitch angle command θ_d in the presence of actuator fault. In this case, it is assumed that the quadrotor helicopter is in a hover mode. The desired pitch command is generated from the following pre-filter [27]:

$$\ddot{\theta}_d + 3\dot{\theta}_d + 4\theta_d = 4\theta^\star, \tag{54}$$

where $\theta^\star$ changes from 0 to 5° at 5 s, and goes back to 0 at 10 s, then changes to −5° at 15 s, and goes back to 0 at 20 s, after that, remains on 0 for 10 s. Three different faulty cases are considered. In the first case, 20% loss of control effectiveness fault occurs in actuator #1 at 14 s. In the second case, 50% loss of control effectiveness fault occurs in actuator #1 at 14 s. Finally, the quadrotor helicopter is commanded to track a circular trajectory, and 50% loss of control effectiveness faults occur in two different actuators at 50 s and 70 s, respectively.

4.1. *Case 1: 20% loss of control effectiveness in one actuator*

For the nominal SMC (NSMC), parameters are chosen as $K_1 = \text{diag}([4\ 4\ 10\ 20\ 20\ 10])$, $K_2 = \text{diag}([4\ 4\ 25\ 100\ 100\ 25])$,

$K_c = [5\ 5\ 10\ 12\ 12\ 10]^T$, $\eta = 0.1$, and $\Phi = 0.1$. For comparison, the same values of K_1, K_2, K_c, and Φ are chosen in the proposed adaptive sliding mode controller.

Figures 3 and 5 show the tracking performance of the pitch angle with the nominal sliding mode controller and the proposed adaptive sliding mode controller, respectively, with 20% loss of control effectiveness in actuator #1. Since the changed elements in matrix $\hat{B}$ have the same absolute value, only the adaptive parameter with positive value is illustrated in Fig. 7, which stops changing when the trajectory of the sliding motion is inside the boundary layer. The simulation results show that, after the occurrence of such a relatively small magnitude of the fault, both sliding mode controllers can make a quick compensation to maintain a good tracking performance. Moreover, the NSMC presents a lesser tracking error than the ASMC. This is achieved by using more control effort as can be observed in Figs. 4 and 6.

Remark 4.1. At the beginning, the actuator fault has been considered for designing the NSMC. If the fault is within the bound, the controller will have a quicker response to it and ensure less tracking error. But in the meantime, in order to accommodate the fault, it will sacrifice more control efforts than the ASMC. This is because, the NSMC uses the robustness of the discontinuous control strategy, and the control gain is chosen to be larger due to the consideration of the presumed fault.

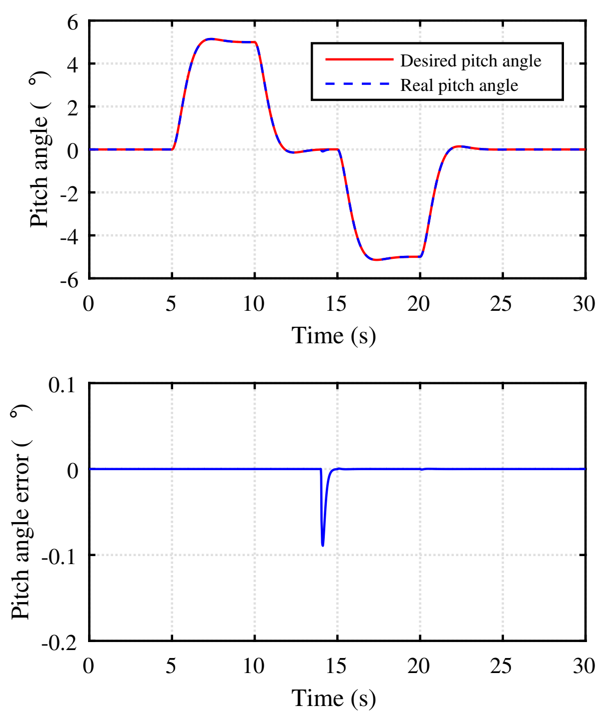

Fig. 3. Tracking performance using NSMC with 20% loss of control effectiveness in actuator #1.

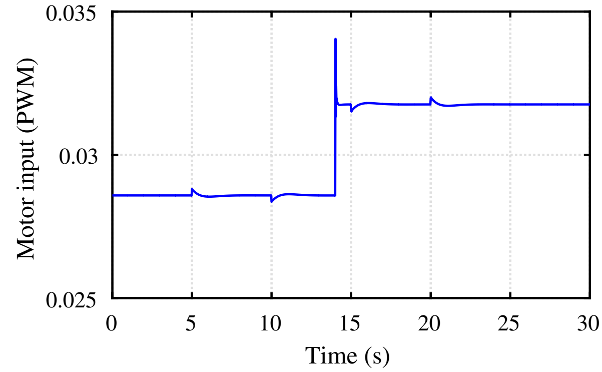

Fig. 4. Control input of the faulty actuator using NSMC with 20% loss of control effectiveness in actuator #1.

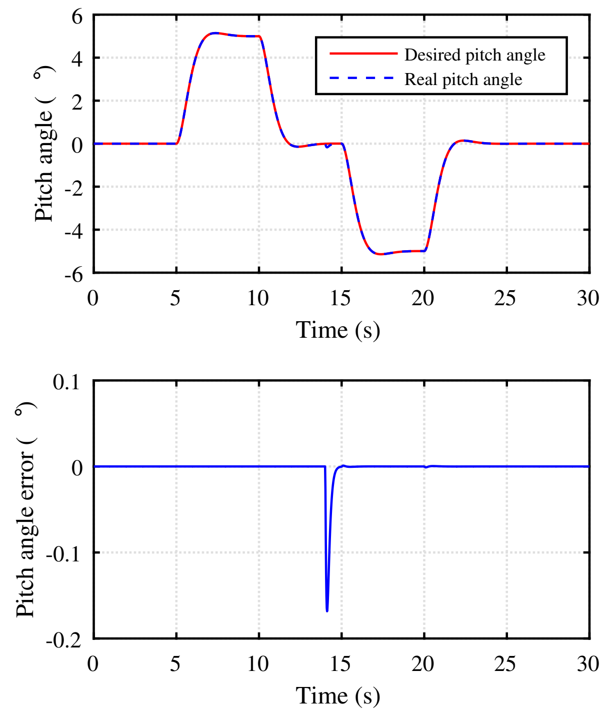

Fig. 5. Tracking performance using ASMC with 20% loss of control effectiveness in actuator #1.

4.2. *Case 2: 50% loss of control effectiveness in one actuator*

In this section, the performance of both controllers are demonstrated when a large fault occurs in actuator #1. In order to maintain the control performance in the fault-free condition, the discontinuous control gain cannot be enlarged ceaselessly. So the gains of both controllers are selected the same as the previous case. 50% loss of control effectiveness fault is now injected at 14 s. As shown in Figs. 8 and 10, for the NSMC, when the actuator fault is increased to 50% loss of control effectiveness, the system

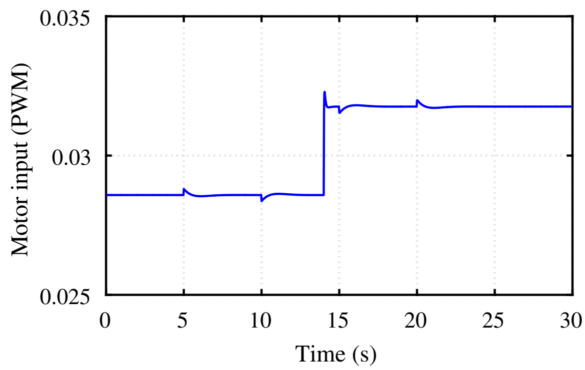

Fig. 6. Control input of the faulty actuator using ASMC with 20% loss of control effectiveness in actuator #1.

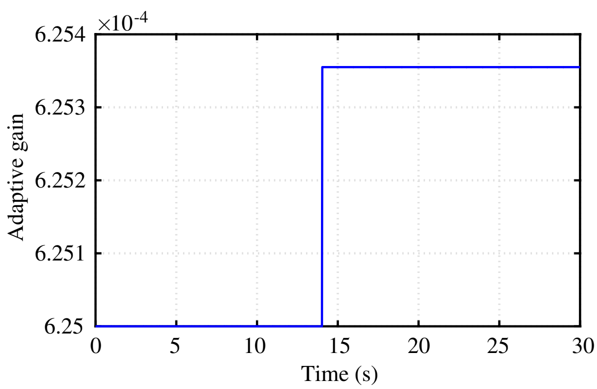

Fig. 7. Adaptive control gain using ASMC with 20% loss of control effectiveness in actuator #1.

still shows a quick response but it cannot track the desired pitch command well with obvious tracking error. What is worse, the chattering appears as shown in Fig. 10. This might stimulate other unmodeled dynamics and make the system performance worse. On the contrary, by using the proposed ASMC, a good tracking performance is maintained and there is only one small overshoot at the initial stage after fault occurrence as shown in Fig. 9. The variation of one of the adaptive elements is shown in Fig. 12, which becomes bigger compared to the one dealing with 20% loss of control effectiveness fault to compensate the larger fault magnitude. As to the control inputs shown in Figs. 10 and 11, the one in the NSMC almost reaches the limit, while the one in the proposed ASMC is maintained much lower. This feature of the proposed ASMC shows its ability of making the system more robust to large uncertainties.

Remark 4.2. During the design stage, if a large fault is considered for NSMC, the system performance cannot be guaranteed in fault-free condition, although it can accommodate a large fault. However, if only a small fault is considered for NSMC in order to maintain system

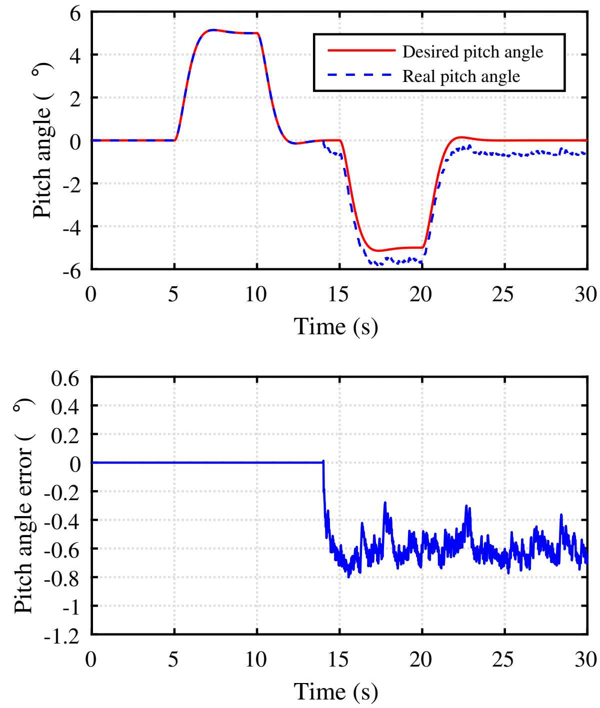

Fig. 8. Tracking performance using NSMC with 50% loss of control effectiveness in actuator #1.

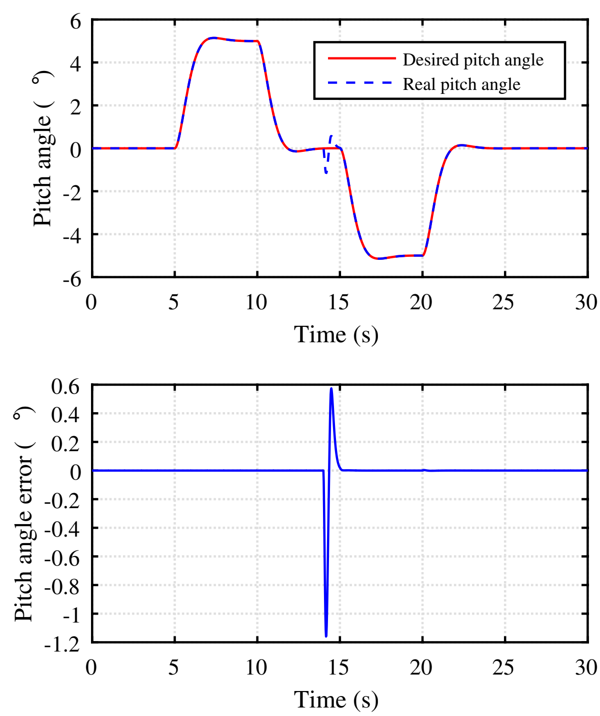

Fig. 9. Tracking performance using ASMC with 50% loss of control effectiveness in actuator #1.

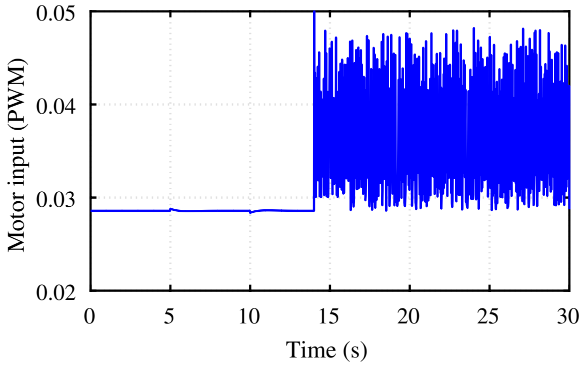

Fig. 10. Control input of the faulty actuator using NSMC with 50% loss of control effectiveness in actuator #1.

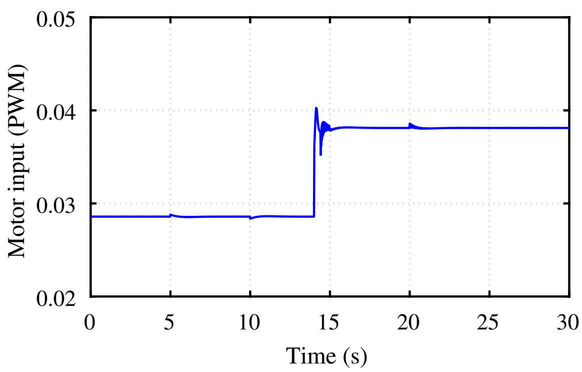

Fig. 11. Control input of the faulty actuator using ASMC with 50% loss of control effectiveness in actuator #1.

performance in both fault-free and faulty conditions, when the uncertainty caused by the fault exceeds the presumed bound, the system performance cannot be maintained anymore. On the contrary, there is no such a worry for the proposed ASMC, and it shows the strong ability of maintaining the system performance seamlessly in the presence of large actuator faults.

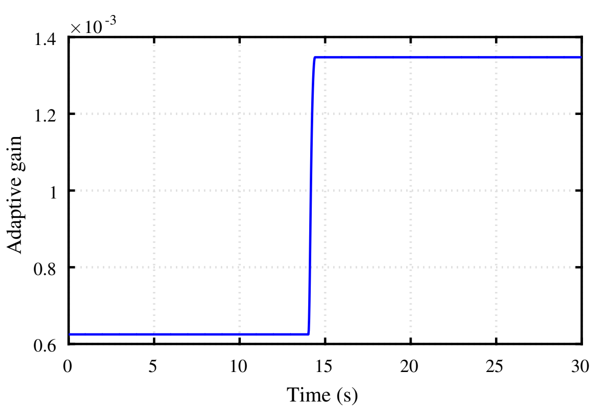

Fig. 12. Adaptive control gain using ASMC with 50% loss of control effectiveness in actuator #1.

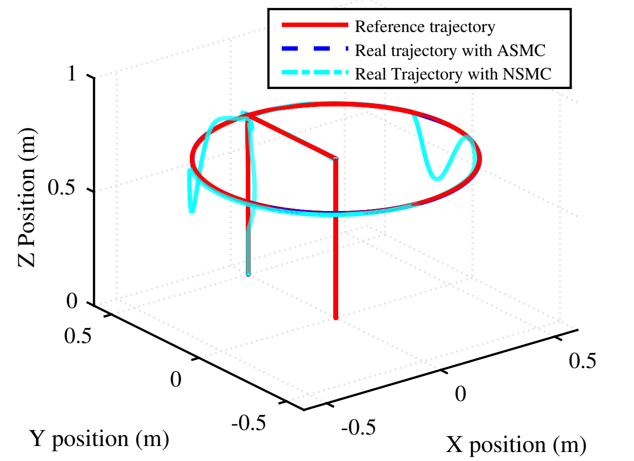

Fig. 13. 3D trajectory tracking with 50% loss of control effectiveness in actuators #1 and #4 sequentially.

4.3. *Case 3*: *3D trajectory tracking with 50% loss of control effectiveness in two different actuators*

In order to demonstrate the effectiveness of the proposed ASMC in the case of multiple different actuator faults

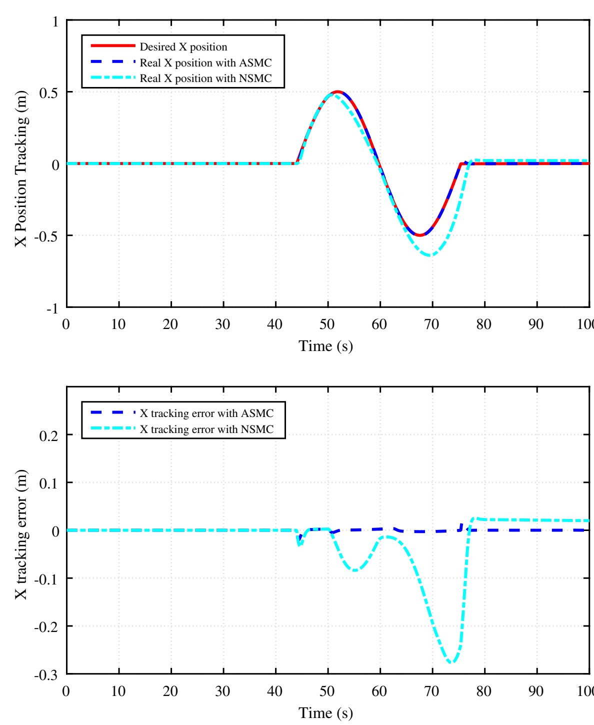

Fig. 14. x position tracking and tracking error with 50% loss of control effectiveness in actuators #1 and #4 sequentially.

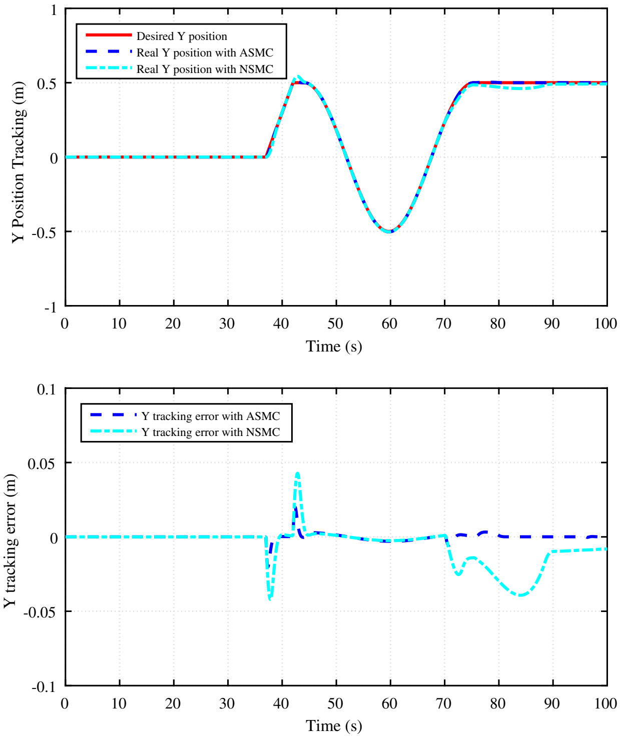

Fig. 15. y position tracking and tracking error with 50% loss of control effectiveness in actuators #1 and #4 sequentially.

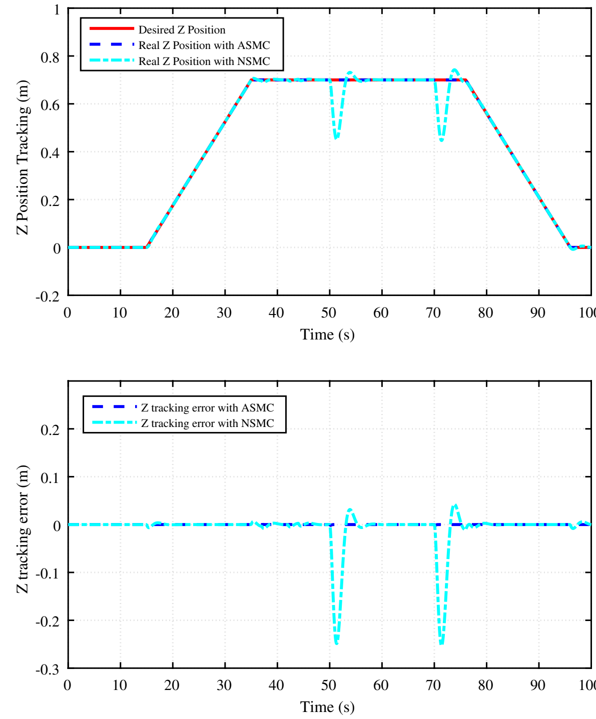

Fig. 16. z position tracking and tracking error with 50% loss of control effectiveness in actuators #1 and #4 sequentially.

occurring in the system, a circular trajectory is commanded to the quadrotor helicopter as shown in Fig. 13. The tracking performance of the NSMC is also shown as comparison. The diameter of the circle is defined as 1 m. Firstly, the quadrotor helicopter is lifted up to 0.7 m, and then it is commanded to move along the y-axis to the tip of the circle. After that, it follows a clockwise circular trajectory. 50% loss of control effectiveness fault occurs in actuators #1 and #4 at 50 s and 70 s, respectively. The detailed translational position tracking performance for each direction is shown in Figs. 14, 15, and 16, respectively, and the inner loop attitude control performance is shown in Figs. 17 and 18, respectively. From the simulation results, it can be seen that, after faults' occurrence, the proposed ASMC can make a quick compensation to maintain the inner loop attitude control, and then it results in a smaller impact on the outer loop position tracking performance.

Remark 4.3. Since the output of the outer loop controller is the desired attitude angle, so there is no direct relationship between the position control and the actuators. Then, for x and y position controls, when an actuator fault occurs, the most important issue is to maintain the inner loop attitude control performance. This is because, as long as the desired attitude angle is tracked, the performance of the whole system is guaranteed.

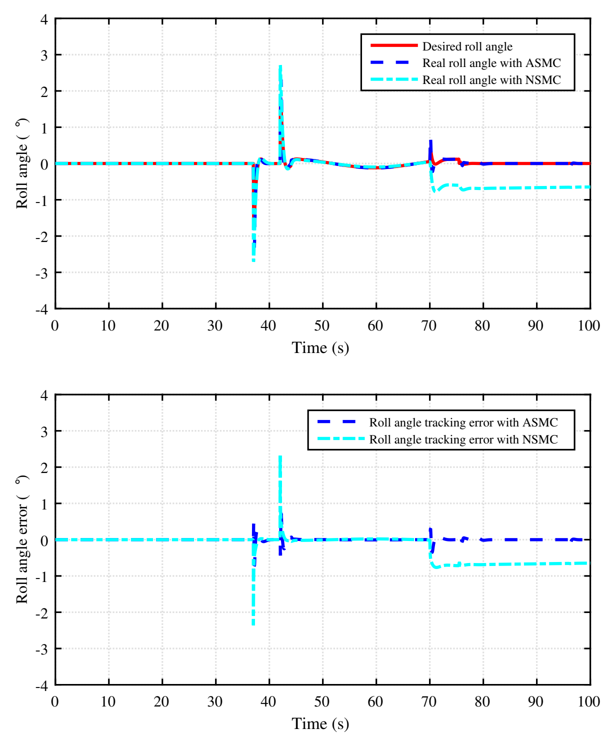

Fig. 17. Roll angle tracking and tracking error with 50% loss of control effectiveness in actuators #1 and #4 sequentially.

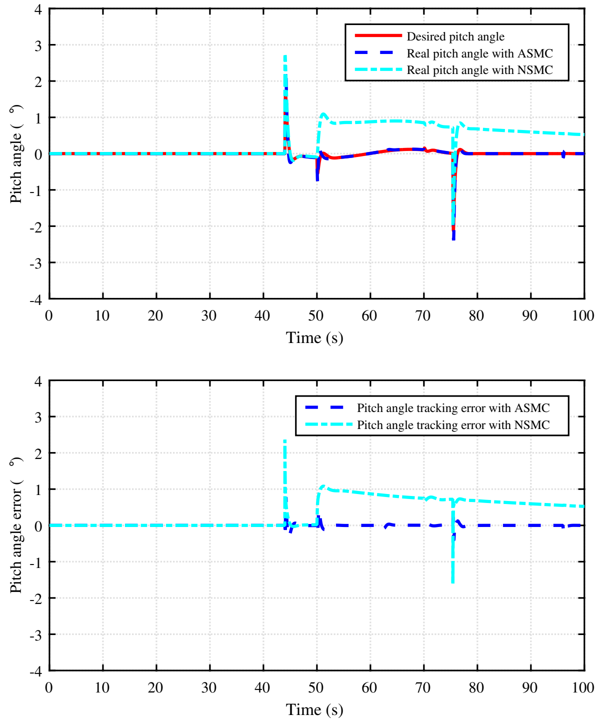

Fig. 18. Pitch angle tracking and tracking error with 50% loss of control effectiveness in actuators #1 and #4 sequentially.

5. Conclusions

In this paper, a novel ASMC method is proposed to control an unmanned quadrotor helicopter in the presence of actuator faults. When faults occur, the proposed ASMC scheme is able to automatically provide robustness and maintain good tracking performance with even a large fault magnitude. The main contribution of the proposed method is that it does not require the bound of the uncertainty to be known. Meanwhile, the control effort is reduced and the chattering phenomenon is eliminated especially when a large fault is considered with the help of the adaptive change of both continuous and discontinuous control parts. The control scheme is validated under different faulty scenarios. The simulation results show that the proposed ASMC achieves a good tracking performance in both fault-free and faulty conditions.

Acknowledgments

This work is supported partially by the scholarships from China Scholarship Council (CSC) (No. 201406290023), NNSFC (No. 61573282), SPNSF (No. 2015JZ020), and NSERC. Thanks to the editors-in-chief, guest editors and all Reviewers for the careful review, constructive comments, and suggestions given during the review process to improve significantly the quality of the paper.

References

[1] G. Pajares, Overview and current status of remote sensing applications based on unmanned aerial vehicles (UAVs), *Photogramm. Eng. Remote Sens.* **81**(4) (2015) 281–329.
[2] K. Nonami, Prospect and recent research & development for civil use autonomous unmanned aircraft as UAV and MAV, *J. Syst. Des. Dyn.* **1** (2) (2007) 120–128.
[3] I. Sadeghzadeh, M. Abdolhosseini and Y. M. Zhang, Payload drop application using an unmanned quadrotor helicopter based on gain-scheduled PID and model predictive control, *Unmanned Syst.* **2**(1) (2014) 39–52.
[4] F. Sharifi, M. Mirzaei, Y. M. Zhang and B. W. Gordon, Cooperative multi-vehicle search and coverage problem in an uncertain environment, *Unmanned Syst.* **3**(1) (2015) 35–47.
[5] Z. Li, Y. Liu, R. Walker, R. Hayward and J. Zhang, Towards automatic power line detection for a UAV surveillance system using pulse coupled neural filter and an improved hough transform, *Mach. Vis. Appl.* **21**(5) (2010) 677–686.
[6] L. Merino, F. Caballero, J. R. Martnez-de Dios, I. Maza and A. Ollero, An unmanned aircraft system for automatic forest fire monitoring and measurement, *J. Intell. Robot. Syst.* **65**(1–4) (2007) 533–548.
[7] C. Yuan, Y. M. Zhang and Z. Liu, A survey on computer vision based technologies for automatic forest fire detection using UAVs and remote sensing techniques, *Can. J. For. Res.* **45**(7) (2015) 783–792.
[8] Z. Liu, C. Yuan, X. Yu and Y. M. Zhang, Fault-tolerant formation control of unmanned aerial vehicles in the presence of actuator faults and obstacles, *Unmanned Syst.* **4**(3) (2016) 197–211.
[9] Y. M. Zhang, A. Chamseddine, C. Rabbath, B. Gordon, C.-Y. Su, S. Rakheja, C. Fulford, J. Apkarian and P. Gosselin, Development of advanced FDD and FTC techniques with application to an unmanned quadrotor helicopter testbed, *J. Franklin Inst.* **350**(9) (2013) 2396–2422.
[10] A. Chamseddine, D. Theilliol, Y. M. Zhang, C. Join and C. A. Rabbath, Active fault-tolerant control system design with trajectory replanning against actuator faults and saturation: Application to a quadrotor unmanned aerial vehicle, *Int. J. Adapt. Control Signal Proc.* **29**(1) (2015) 1–23.
[11] Z. Liu, C. Yuan, Y. M. Zhang and J. Luo, A learning-based fault tolerant tracking control of an unmanned quadrotor helicopter, *J. Intell. Robot. Syst.* **84**(1–4) (2016) 145–162.
[12] Y. M. Zhang and J. Jiang, Bibliographical review on reconfigurable fault-tolerant control systems, *Annu. Rev. Control* **32**(2) (2008) 229–252.
[13] X. Yu and J. Jiang, A survey of fault-tolerant controllers based on safety-related issues, *Annu. Rev. Control* **39** (2015) 46–57.
[14] C. Edwards, T. Lombaerts and H. Smaili, *Fault Tolerant Flight Control: A Benchmark Challenge* (Springer, 2010).
[15] M. Chadli, S. Aouaouda, H. R. Karimi and P. Shi, Robust fault tolerant tracking controller design for a VTOL aircraft, *J. Franklin Inst.* **350**(9) (2013) 2627–2645.
[16] M. Steinberg, Historical overview of research in reconfigurable flight control, *Proc. Inst. Mech. Eng. G J. Aerosp. Eng.* **219**(4) (2005) 263–275.
[17] B. Xiao and S. Yin, Velocity-free fault-tolerant and uncertainty attenuation control for a class of nonlinear systems, *IEEE Trans. Ind. Electron.* **63**(7) (2016) 4400–4411.

[18] R. A. Hess and S. R. Wells, Sliding mode control applied to reconfigurable flight control design, *J. Guid. Control Dyn.* **26**(3) (2003) 452–462.

[19] C. Edwards, H. Alwi and M. T. Hamayun, Fault tolerant control using integral sliding modes, in *Proc. European Control Conf.* Strasbourg, France (2014), pp. 12291–2296.

[20] T. Wang, W. Xie and Y. M. Zhang, Sliding mode reconfigurable fault tolerant control for nonlinear aircraft systems, *J. Aerosp. Eng.* **28**(3) (2015) 04014086.

[21] T. Li, Y. M. Zhang and B. W. Gordon, Passive and active nonlinear fault-tolerant control of a quadrotor unmanned aerial vehicle based on the sliding mode control technique, *Proc. Inst. Mech. Eng. I J. Syst. Control Eng.* **227**(1) (2013) 12–23.

[22] H. Alwi and C. Edwards, Fault tolerant longitudinal aircraft control using non-linear integral sliding mode, *IET Control Theory Applic.* **8**(17) (2014) 1803–1814.

[23] M. T. Hamayun, C. Edwards and H. Alwi, A fault tolerant control allocation scheme with output integral sliding modes, *Autom.* **49**(6) (2013) 1830–1837.

[24] J. Zhang, X. Liu, Y. Xia, Z. Zuo and Y. Wang, Disturbance observer-based integral sliding-mode control for systems with mismatched disturbances, *IEEE Trans. Ind. Electron.* **63**(11) (2016) 7040–7048.

[25] Q. Hu and B. Xiao, Adaptive fault tolerant control using integral sliding mode strategy with application to flexible spacecraft, *Int. J. Syst. Sci.* **44**(12) (2013) 2273–2286.

[26] J. He, R. Qi, B. Jiang and J. Qian, Adaptive output feedback fault-tolerant control design for hypersonic flight vehicles, *J. Franklin Inst.* **352**(5) (2015) 1811–1835.

[27] T. Wang, W. Xie and Y. M. Zhang, Sliding mode fault tolerant control dealing with modeling uncertainties and actuator faults, *ISA Trans.* **51**(3) (2012) 386–392.

[28] B. Wang, K. A. Ghamry and Y. M. Zhang, Trajectory tracking and attitude control of an unmanned quadrotor helicopter considering actuator dynamics, in *Proc. 35th Chinese Control Conf. (CCC)* (IEEE, 2016), pp. 10795–10800.

[29] Q. I. Educate, Quanser Qball-X4 user manual (2007).

Ban Wang received his B.S. and M.S. degrees from the Northwestern Polytechnical University, Xi'an, China, in 2011 and 2014, respectively. He is currently working towards the Ph.D. degree at the Department of Mechanical, Industrial and Aerospace Engineering, Concordia University, Montreal, Canada. His research interests include fault-tolerant flight control, fault detection and diagnosis, and cooperative control of unmanned aerial vehicles.

Youmin Zhang received his B.S., M.S., and Ph.D. degrees from the Northwestern Polytechnical University with specialization in automatic controls, Xi'an, China, in 1983, 1986, and 1995, respectively.

He is currently a Professor at the Department of Mechanical, Industrial and Aerospace Engineering and the Concordia Institute of Aerospace Design and Innovation (CIADI) at the Faculty of Engineering and Computer Science of Concordia University, Canada. His main research interests and experience are in the areas of condition monitoring, health management, fault diagnosis and fault-tolerant (flight) control systems; cooperative guidance, navigation and control of unmanned aerial/space/ground/surface vehicles with applications to forest fires, pipelines, power lines, environment, natural resources and natural disasters monitoring, detection, and protection by combining with remote sensing techniques; dynamic systems modeling, estimation, identification and advanced control techniques; and advanced signal processing techniques for diagnosis, prognosis, fault-tolerant and health management of safety-critical systems with application to renewable and hybrid energy systems and smart grids, and manufacturing processes. He has published four books, over 430 journal and conference papers, and book chapters. He has been invited to deliver plenary talks at international conferences/workshops and research seminars worldwide for more than 90 times. He is a fellow of CSME, a senior member of AIAA, a senior member of IEEE, a member of Technical Committee (TC) for several scientific societies, including the IFAC TC on Fault Detection, Supervision and Safety for Technical Processes, the AIAA Infotech@Aerospace Program Committee (PC) on Unmanned Systems, IEEE Robotics and Automation Society TC on Aerial Robotics and Unmanned Aerial Vehicles, ASME/IEEE TC on Mechatronics and Embedded Systems and Applications, and a member of ICUAS Association Executive Committee. He is a founding Editor-in-Chief of the Journal of Instrumentation, Automation and Systems, an Editor-at-Large of the Journal of Intelligent & Robotic Systems, and an Editorial Board Member/Associate Editor of several other international journals (including three newly launched journals on Unmanned Systems). He has served as General Chair, Program Chair, Program Vice Chair, and IPC Member of several international conferences, including the General Chair of the 10th International Conference on Intelligent Unmanned Systems (ICIUS) in 2014, Montreal, Canada, Program Chair of the International Conference on Unmanned Aircraft Systems (ICUAS) in 2014, Orlando, USA, one of General Chairs of the ICUAS in 2015, Denver, USA, a Co-General Chair of the ICIUS 2016 held at Xian, China, a Program Co-Chair for the SDPC 2017, Shanghai, China, Program Chair of the ICUAS 2017 held at Miami, USA, and General Chair of the ICUAS 2018 to be held at Dallas, USA during June 12-15, 2018. More detailed information can be found at http://users.encs.concordia.ca/˜ymzhang/.